Received: 12 June 2020 | Revised: 30 January 2021 | Accepted: 8 March 2021

DOI: 10.1049/rpg2.12174

IET Renewable Power Generation

The Institution of Engineering and Technology WILEY

ORIGINAL RESEARCH PAPER

Modelling battery energy storage systems for active network management—coordinated control design and validation

Chethan Parthasarathy[1] | **Katja Sirviö**[1] | **Hossein Hafezi**[2] | **Hannu Laaksonen**[1]

[1] School of Technology and Innovation, Flexible energy resources, University of Vaasa, Yliopistoranta 10, Vaasa, Finland

[2] Faculty of Information Technology and Communication Sciences, Tampere University, Tampere, Finland

Correspondence
Chethan Parthasarathy, School of Technology and Innovation, Flexible energy resources, University of Vaasa, Yliopistoranta 10, Vaasa, Finland.
Email: chethan.parthasarathy@uwasa.fi

Abstract

Control of battery energy storage systems (BESS) for active network management (ANM) should be done in coordinated way considering management of different BESS components like battery cells and inverter interface concurrently. In this paper, a detailed and accurate lithium-ion battery model has been used to design BESS controls, thereby allowing improved overall power system control design optimisation studies by simultaneously considering both component and system-level aspects. This model is utilised to develop a multi-objective ANM scheme (a) to enhance utilisation of wind power generation locally by means of active power (*P*)- control of BESSs; (b) to utilise distributed energy resources (i.e. BESS and wind turbine generators) to maintain system voltage within the limits of grid code requirements by reactive power/voltage (*QU*)- and active power/voltage (*PU*)- controls. BESS control strategies to implement the ANM scheme, are designed and validated through real-time simulation in an existing smart grid pilot, Sundom Smart Grid (SSG), in Vaasa, Finland.

1 | INTRODUCTION

The stochastic and unpredictable nature of the renewable energy sources (RES) and their geographic location, often in remote areas with weak electrical grids, present upcoming network issues, where relatively small-sized RESs are connected to the power grid in the LV/MV distribution systems. Managing power balance and power system stability (especially system voltages) is a challenging task in such situations. Therefore, innovative ANM schemes designed to manage available flexibilities in the LV/MV distribution system play a pivotal role in raising the network RES hosting capacity and managing different network parameters (voltage, reactive power flow and frequency) within the threshold values dictated by grid codes.

RES based distributed energy resources (DERs) in the MV and LV distribution network play an important role in providing flexibility in the power system for local and system-wide grid resiliency, and maximising network DER hosting capacity [1–3]. These flexibilities consist of active power (*P*-) and reactive power (*Q*-) control of flexible resources, such as, controllable DER units, battery energy storage system (BESS), controllable loads and electric vehicles (EVs) which are connected in distribution system operator's (DSOs) grids providing different local and system-wide technical services as part of future ANM schemes [4–8].

ANM principles in [4–6] were modelled to dispatch flexibilities in the distribution system for the day-ahead market through mathematical optimisation techniques. Whereas, [7, 8] consider voltage regulation by means of reactive power control considering DER power capability curve limits and grid codes in an existing MV grid. Such studies provide details on the overall *P*- and *Q*-optimal dispatch for RESs and BESSs in the LV/MV distribution systems. However, network management studies considering the effect of such optimal dispatch on the operation of DERs and their grid-side and/or component level controllers are minimal. Considering the economic and technical aspects of DERs, especially BESSs, it is imperative to model their performance characteristics in detail.

BESSs because of their fast and controllable dynamics have the potential to provide multiple different flexibility services in stationary grid applications, especially in the ANM schemes acting as a buffer, to manage flexibilities in the distribution

systems. From transmission and distribution system operators (TSO/DSOs) point of view, an effective way to utilise BESSs for ANM, will be to place them in an HV/MV substation or the MV distribution for example at MV/LV substations. Their benefits [9] include,

1. Increase the capacity to transfer active power by storing the energy at times of higher RES generation, avoiding the cost for additional transfer capacity
2. Secure reliable LV-network distribution to all or the most critical customers in cases of MV-network fault by utilising intended island operation
3. The storage capacity of MV/LV substations can be increased in a modular way for example, when customer reliability requirements or RES integration in LV network increase
4. Local compensation of reactive power produced by underground cables by decreasing the reactive power exchange in the MV network, thereby reducing network losses and increasing active power flow
5. Continuously control reactive power flow through the distribution system to minimise frequent tap changes in OLTC when the amount of flexibilities is higher in a system [10]

In addition to local flexibility services, BESSs can also provide a variety of system-level technical ancillary/flexibility services [9]. The utilisation of BESSs for single purpose such as improving electricity supply reliability (intended islanded or microgrid operation) or increasing RES penetration in the distribution network may not be economically viable, considering its robust ability to participate in multi-use case scenarios [11]. Hence, the developed ANM scheme is based on the multi-use capability of BESSs.

Lithium-ion (Li-ion) BESSs are capable of acting as flexible energy sources and providing multiple technical ancillary/flexibility services including frequency support by controlling active power injection and voltage regulation by reactive power control [12–14]. Ability to react fast, higher energy and power density, longer cycle and shelf life, low self-discharge rate, high round trip efficiency and improved safety performance have favoured Li-ion based BESSs for stationary grid applications. However, Li-ion batteries are intercalation-based energy storage systems, which operate as a closed system [15] with very few measurable state variables, which makes it difficult to monitor the states of the battery properly. Therefore, it is required to understand model precisely the Li-ion BESS behaviour under various operating conditions, unlike in recent research [16–18], where generic or most basic Li-ion battery models are considered.

In this paper, the equivalent circuit model (ECM) is developed for nickel-manganese-cobalt-oxide (NMC) cathode based Li-ion battery and used to design BESS control topologies. In terms of performance, ECMs are highly accurate than the kinetic battery models (KBM)/modified KBMs [19, 20] and mathematical models [21]. ECMs [22–26] are computationally less intensive compared to the Physics-based electrochemical models [27]. In this study, second-order equivalent circuit (SOEC) of Li-ion BESSs has been proposed and placed strategically in the MV distribution grid harnessing its utilisation for multi-objective ANM scheme.

In order to maximise the multi-use capabilities of BESSs for distribution systems, controllers such as reactive power/voltage (*QU-*), active power/voltage *(PU-)* and active power (*P-)* controls are designed to act in co-ordination with each other. In previous research [28, 29], BESS integration to the MV bus of SSG was studied in detail considering the fast dynamics of the power systems, where the grid was modelled in EMT mode capturing the power system fast transients in detail. However, the slow dynamics that is control of voltages over an extended time will be modelled in the scope of this paper. Overall, in this paper, the focus was laid on,

1. Development of ANM architecture with *QU-, PU-* and *P-*controllers for managing available flexibilities of various DERs, especially to generate control signals for the BESS and wind turbine generator (WTG) inverters in the MV distribution system
2. The utilisation of accurate ECM for Li-ion BESS controller development in grid integration studies
3. Studying the effects of BESS inverter operation on the Li-ion BESS performance, including the thermal effects of Li-ion batteries
4. Understanding the interaction of BESS inverter controller with the grid side controllers in the distribution system

In this paper, the SOEC model for Li-ion BESS grid integration studies includes *SoC*, temperature, current rate and ageing effects explained in Section 2. The ANM architecture to manage flexible energy sources and its underlying controller design for a stable MV distribution system is presented in Section 3. Validation of the developed ANM scheme is implemented in Section 4, by managing the available flexibilities in MV distribution system in SSG network.

2 | LI-ION BATTERY MODEL

Thevenin-based SOEC model is a versatile technique [25]. It successfully emulates the model parameters such as multivariable *SoC*, charge-rate (C-rate), temperature, hysteresis effects, self-discharge and battery ageing. SOEC is considered the benchmark model for Li-ion batteries, as it depicts the charge transfer, diffusion and solid electrolyte interface reactions in the form of resistors and capacitors.

Figure 1 shows the proposed dynamic equivalent circuit model for the NMC type Li-ion battery cell. Open circuit voltage (OCV) is modelled as an ideal voltage source, and the internal resistance is modelled as R_i. Two RC combinations are suggested for modelling Li-ion battery cell, so that the dynamic behaviour is modelled as R_1, C_1, R_2 and C_2. The hysteresis and polarization effects in the Li-ion cells can be simulated accurately enough with the two RC combinations. The model structure is simpler compared to more RC combinations. The model parameters (OCV, R_i, R_1, C_1, R_2 and C_2) are obtained by hybrid pulse power characterization (HPPC) tests [30].

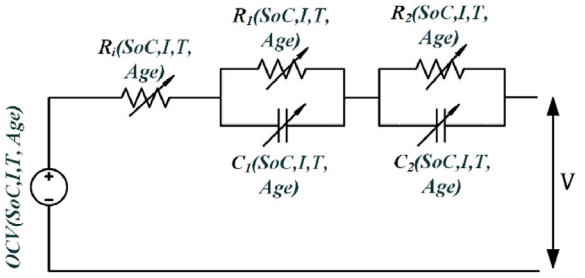

FIGURE 1 SOEC battery cell model

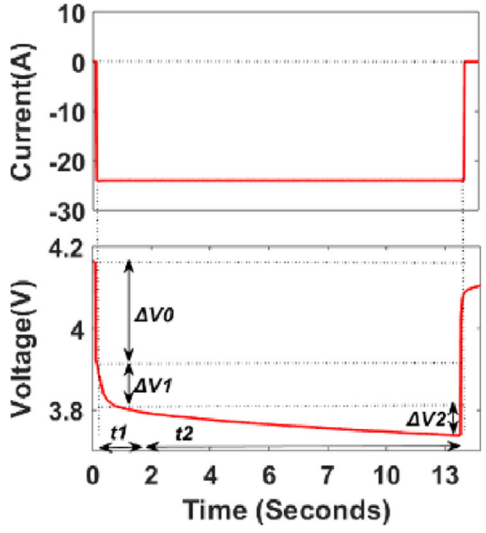

FIGURE 2 HPPC test response at 100% SoC and 25 °C

A closer view of the voltage response from the HPPC profile can be seen in Figure 2. It shows an immediate voltage drop (ΔV_0) when the current pulse (I) is applied. This result is the internal resistance of the cell, which is contributed by resistance of active material, electrolyte and current collector. It can be also observed that there is a time-varying voltage (ΔV_1 and ΔV_2), which can be interpreted as a presence of additional elements such as a capacitor in parallel combination with resistance. The time-varying voltage part can be divided into short transient and long transient RC elements due to different time constants (t_1 and t_2) in the voltage profile. The output voltage equation for the second order ECM is shown Equation (1). The mathematical representation of the time constants is shown in Equations (2) and (3). OCV is evaluated from the voltage response of the HPPC profile at a given *SoC* interval, at the end of 1 h pause time.

SoC is estimated by using coulomb counting method (CC) [26]. CC method provided the best accuracy with minimal computational effort in an environment where the measurement noise was minimal [31], such as measurements from battery cyclers. Hence, the *SoC* calculation from the CC method has been considered as the reference value in this study. The overall performance of the SOEC battery model is depicted in Figure 3 by comparing experimental and simulated voltage curves using the HPPC load current profile.

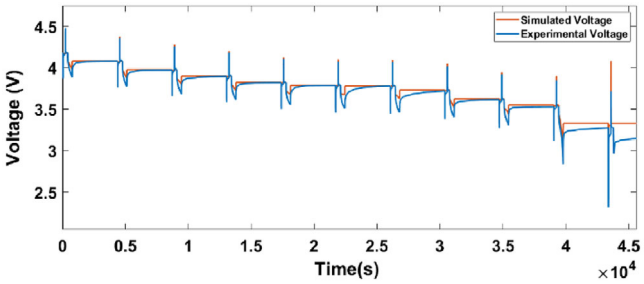

FIGURE 3 Battery model performance (HPPC profile)

The SOEC modelling technique can be utilised to estimate heat generated by battery cell, which leads to the temperature increase due to Joule heating effect. This temperature change affects the performance of the Li-ion battery considerably [13]. The major highlight between the model developed in [30] and the model presented in this paper is the development of the thermal model, which considers both *SoC* and inner cell temperature as affecting parameters. The inner cell temperature is considered uniform within the cell and taken as the average temperature inside the cell. Equation (4) represents the irreversible heat generated by the battery cell due to the Joule effect [32]. Therefore, temperature changes during the cell operations are determined providing set points for the thermal cooling system and the battery management system.

$$V_T(t) = V_{OCV} + I(t)R_i + I(t)R_1\left(1 - e^{\frac{-t}{t1}}\right) + I(t)R_2\left(1 - e^{\frac{-t}{t2}}\right) \quad (1)$$

$$t_1 = R_1 C_1 \quad (2)$$

$$t_2 = R_2 C_2 \quad (3)$$

$$P_{th}(t) = R_i(SoC, T_b) I^2(t) = m_b C_p \frac{dT_b}{dt} + P_a(t) \quad (4)$$

where,

m_b: mass of the battery [Kg]
C_p: Specific heat capacity of the battery [J/Kg K]
T_b: Uniform Temperature inside the battery [K]
P_a: Heat transfer rate to the cooling system [W]
P_{th}: Heat generated in battery due to Joule effect

3 | ACTIVE NETWORK MANAGEMENT

In [33–36] extensive research on various ANM schemes to maintain system voltage by control of reactive power flow from the DERs within the reactive power window (RPW) provided by the Finnish TSO, Fingrid and ENTSO-E standards have been studied and validated in a local smart grid pilot SSG. RPW

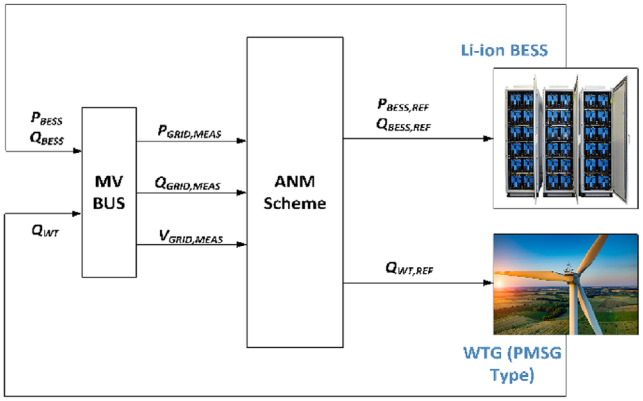

FIGURE 4 Flexibility management schematic in SSG MV grid

specified by Fingrid at the HV side of the TSO/DSO interface is represented in [36] and the requirement at the MV side is presented in [37]. The maximum active power limits are based on the measured data from year 2016, when imported grid power was 8.3 MW and the exported was 1.975 MW. According to the grid codes, the ANM voltage control is set to a maximum voltage of 1.05 pu, and the minimum voltage limits are set at 0.95 pu (both HV and MV connection points), which is based on the thermal limit for maximum current flow in the system. From previous results, the reactive power control of WTG was adequate to satisfy RPW conditions. However, it was recommended to study multi-use capabilities of BESSs such as, active power control flexibility, primarily to improve RES hosting capacity and reactive power control utilisation to complement WTG

Proposed flexibility management schematic for the MV grid of SSG is shown in Figure 4. The ANM architecture developed in Section 3.1, forms the basis to deploy flexibility management in the MV distribution system. The ANM scheme in-turn depends on the functionalities of the energy management system (EMS) and its adjoining controllers to provide technical ancillary services. Details of the ANM architecture, EMS functionalities and the EMS controller design to provide flexibility management is explained further in this section.

3.1 | Active network management architecture with BESS

BESSs integrated to the SSG MV bus are primarily designed to complement the stochastic nature of wind power generation, that is, store excess wind power generation and discharge during reduced wind power generation. Secondly, they are used to provide technical ancillary services. The WTG primarily caters maintaining the HV side of the grid within the RPW. However, the reactive power (Q_{WT}) control flexibilities provided by the WTG are dependent on the active power generation (P_{WT}), which in turn is dependent on the intermittent nature of wind. There by, WTG alone may not be sufficient to provide flexibilities in a power system, especially with respect to the reactive power compensation by the WTG. Hence, BESS placed strategically in the MV distribution grid will be able to complement WTG in providing various technical services in the MV distribution side of the smart grid.

The ANM control architecture described in Figure 5 was designed to implement in SSG to manage flexibilities offered by WTG and Li-ion BESS. Enhancing local utilisation of wind power generation with the aid of BESSs is the primary objective of this ANM architecture. Voltage regulation within the threshold in the MV side of the grid constitutes the secondary objective. Measured MV grid data, that is active power ($P_{GRID,MEAS}$), reactive power ($Q_{GRID,MEAS}$) and voltages ($V_{GRID,MEAS}$) is provided as the input to the control architecture. The first layer in the control architecture consists of different control techniques, capable of providing technical services to enforce ANM. *QU-*, *P-* and *PU*-control methodologies helps in managing different available flexibilities in the power system. In this layer, the total required reactive power control is required to maintain targets for RPW control and *QU*-control, the Fingrid codes' requirements, thereby defining the overall requirements for *QU*-control of flexible energy sources. Along with that, the *P*-control for BESSs is estimated and dispatched to the next layer. *PU*-control requirements are calculated when *QU*-control does not satisfy the grid code requirements.

The next layer of operation in the ANM scheme is the EMS which concerns with the operation of active and reactive power flows from the flexible energy sources, in this case BESS and WTG. Grid requirement references such as $Q_{\mathrm{GRID,REF}}$, $P_{\mathrm{BESS,REF}}$ and $P_{\mathrm{GRID,REF}}$ are given as input to the EMS layer, where it distributes the related operations to the BESS and WTG based on the availability of their individual flexibilities. Therefore, based on Equations (5)–(9), EMS generates reference values $Q_{\mathrm{BESS,REF}}$ and $P_{\mathrm{BESS,REF}}$ to the BESS and $Q_{\mathrm{WT,REF}}$ and $P_{\mathrm{GRID,REF}}$ to the WTG. Based on the internal control algorithms for BESS and WTG defined in the following section, BESS returns relevant P_{BESS} and Q_{BESS} to the EMS, whereas WTG returns Q_{WT} to the EMS.

These control signals are then forwarded to the EMS controllers as Q_{FLEX} (Q_{BESS} and Q_{WT}) to the *QU*-controller, P_{BESS} is forwarded to the P-controller and P_{FLEX} is provided to the *PU*-controller layers. All the three control layers act in tandem to provide $Q_{GRID,Flex}$ and $P_{GRID,Flex}$ to the MV grid, there by controlling the active and reactive power flows in the HV/MV connection point regulating the values based on the RPW control requirements.

Figure 6(a–c) shows the design and architecture of the individual control techniques, that is *QU-*, *P-* and *PU*-controls respectively employed in the ANM management principle defined. Their overall operations are explained as below.

3.1.1 | *QU*-management system

Voltage regulation at the MV side (V_{MV}) of the HV/MV connection point is the primary objective of this control loop by

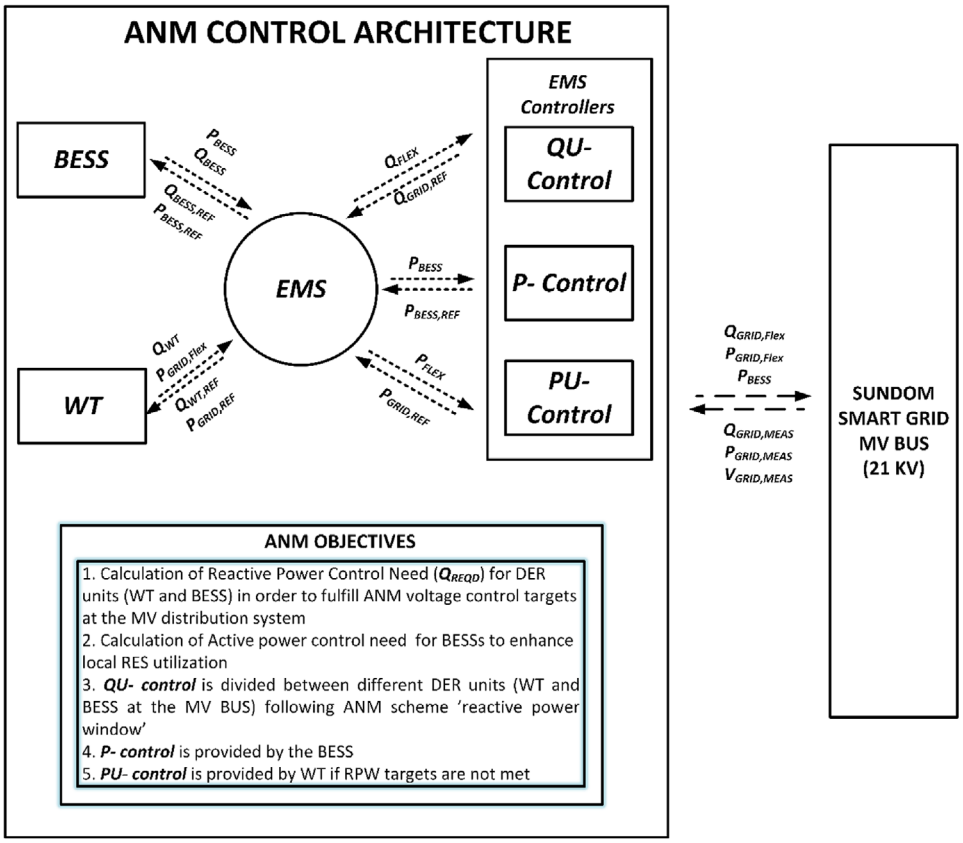

FIGURE 5 ANM scheme and its adjoining EMS controller operations

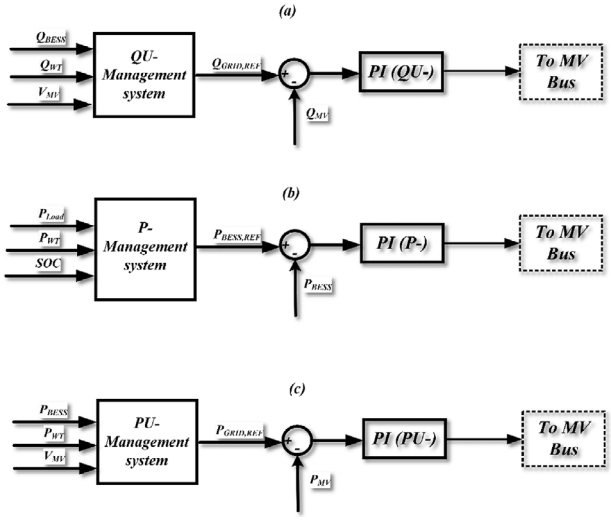

FIGURE 6 (a) *QU*-control, (b) P-control and (c) PU-control

controlling the available flexibilities (i.e.Q_{WT} and Q_{BESS}) when its voltage falls below 0.95 p.u. The decoupling between reactive power control and the active power control of the distributed energy sources in this case WTG and BESS have to be clearly defined to avoid controller interactions. Hence, for both the DERs when in *QU*-control mode, their maximum possible reactive power support is taken into account by the control algorithms.

Q_{WT} control of WTG system depends on the reactive power output capability. The inverter operating range should be applied accurately before utilising reactive power control strategy in WTGs so that the maximum active power generation from the wind turbine is not disturbed. Therefore, the maximum controllable reactive power from the WTG is calculated by Equation (5). $Q_{WT,min}$ and $Q_{WT,max}$ are the maximum and minimum reactive power output from the WTG. S_{WT} denotes apparent power of the WTG. The negative symbol denotes absorbing reactive power and that of positive symbol to generate reactive power.

P-control of the BESS was set higher in the hierarchy so that its main goal is to enhance wind power penetration by controlling the charging and discharging P_{BESS} as per the grid's requirement. However, the reactive power control of BESS is defined by the phasor relationship between the battery inverter operating parameters as in Equation (6), for several different levels of BESS active power output (P_{BESS}). When S_{BESS} is larger than P_{BESS}, the inverter can supply or consume reactive power, Q_{BESS} . The BESS inverter can dispatch Q_{BESS} quickly (on the cycle-to-cycle time scale) providing a mechanism for rapid voltage regulation. As the output,P_{BESS} approaches S_{BESS} (apparent power of Li-ion BESS), the range of available Q_{BESS} decreases to zero.

3.1.2 | *P*-management system

Due to its capability in catering both active and reactive power requirements of the SSG, BESS control includes both *P*-control by regulating P_{BESS} and *QU*-control by regulating Q_{BESS}, there by satisfying the ANM requirements commanded by the MV distribution system in SSG.

Li-ion BESS active power control in the MV distribution system shown in Equation (7), which is primarily designed to charge (P_{chg}), when the wind power generation exceeds load demand and discharge power (P_{dis}) during higher demand than its wind power production, which is controlled by the battery's *SOC* within their threshold SOC_{min} and SOC_{max}. Overall active power discharged by the BESS is defined by Equation (8) and the BESS is charged with a power of 500 kW as with a C-rate of 0.5 C as shown in Equation (9).

$$Q_{WT,\min} \le Q_{WT} \le Q_{WT,\max}$$

$$\text{where, } \begin{cases} Q_{WT,\min} = -\sqrt{{S_{WT}}^2 - {P_{WT}}^2} \\ Q_{WT,\max} = \sqrt{{S_{WT}}^2 - {P_{WT}}^2} \end{cases} \tag{5}$$

$$Q_{BESS,\min} \le Q_{BESS} \le Q_{BESS,\max}$$

$$\text{where, } \begin{cases} Q_{BESS,\min} = -\sqrt{{S_{BESS}}^2 - {P_{BESS}}^2} \\ Q_{BESS,\max} = \sqrt{{S_{BESS}}^2 - {P_{BESS}}^2} \end{cases} \tag{6}$$

$$P_{BESS} = \begin{cases} P_{dis}; (if\ SOC_{\min} < SOC \langle SOC_{\max}\ and\ P_{Load} \rangle P_{WT}) \\ P_{chg}; (if\ SOC < SOC_{\min}\ and\ P_{WT} > P_{Load}\ ;) \\ 0 \end{cases} \tag{7}$$

$$P_{dis} = P_{Load} - P_{WT} \tag{8}$$

$$P_{chg} = 0.5C \tag{9}$$

3.1.3 | *PU*-management system

PU-management system is designed to keep in mind the curtailment of renewable energy generation, when the voltage limits exceed 1.05 pu in the system's MV bus. To manage the curtailment droop control referred in Figure 7 is utilised for the curtailment of wind power generation.

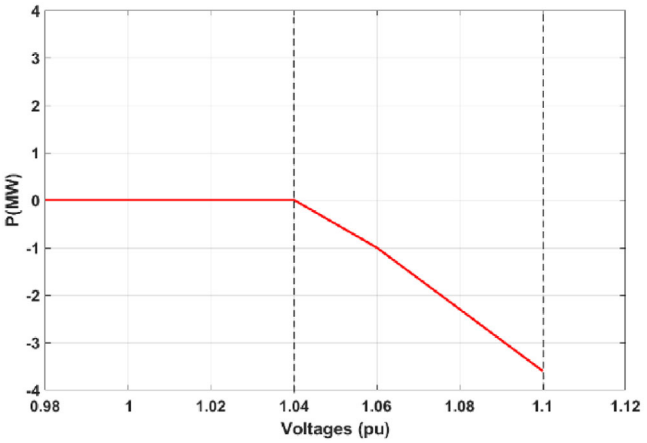

FIGURE 7 PU-droop settings

4 | RESULTS AND DISCUSSION

Dynamic voltage stability simulation is the key component in control and dynamic security assessment tools. The ultimate goal in this field has always been to perform these simulations as fast as real-time for realistic power systems. However, mathematical modelling and numerical solutions are computationally heavy for large-scale systems. On the other hand, continuous growth in electricity demand and the consequent expansion of power grids create new and complex problems. Thus, real-time simulations offer methods for quick and efficient simulations of large-scale systems that are necessary.

To ensure secure functioning of BESSs in smart grids, extensive real-time phasor simulations, where active and reactive power control system design and validation of BESSs over an extended period (i.e. hours to a day) are necessary. They provide accurate setpoints for the battery system controllers. Such simulations are equivalent to developing and verifying secondary and tertiary controllers for BESSs, in a hierarchically controlled power system topology. In this paper, the ANM scheme defining the role of BESS in enhancing wind power generation and MV distribution system voltage control is explored through simulation studies in the ePhasorSim platform by OPAL-RT [38].

ePhasorSim is a real-time transient stability solver used for simulating slow dynamics of large scale power systems in real-time. This tool is interfaced with Matlab/Simulink and compatible with load flow and dynamic data files from PowerFactory simulation software. Hence, for this study SSG model was developed in PowerFactory by the data provided by Local DSO, Vaasan Sähkoverkko and later imported to OPAL-RT to integrate BESSs and design their controllers. Three cases are designed to study the utilisation of available flexibility for ANM of the SSG, predominantly voltage control and better utilisation of wind power generation. None of the flexibilities are utilised in the first case, thereby providing the base case scenario used to compare second (WTG as flexibility source) and third case (WTG and BESS as flexibility sources). All the simulations run for a period of 24 h, mainly in order to evaluate the different controls of flexible energy sources and their planning over a period of one full day. In all the cases, SSG is modelled as a grid-connected microgrid, without on-load tap changer (OLTC) in the HV/MV transformer. Therefore,

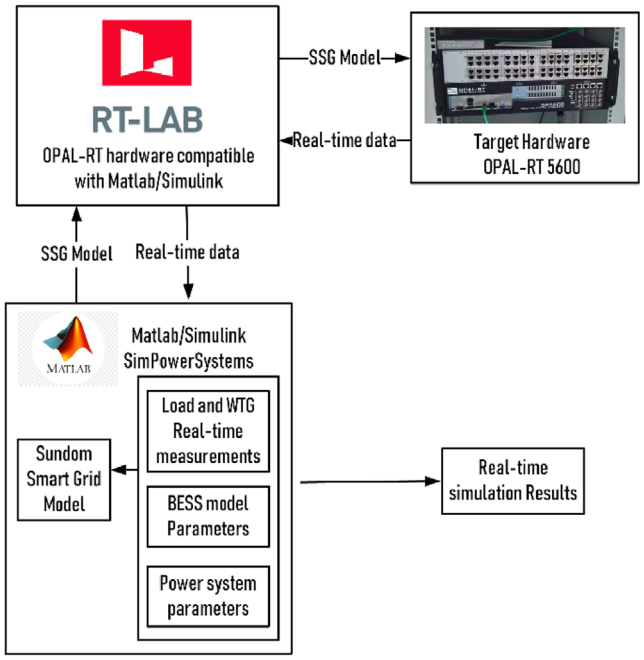

FIGURE 8 SSG real-time simulation set-up

relying on flexibility services available in the grid for voltage regulation.

4.1 | Case 1: Without ANM

The real-time simulation environment is presented in Figure 8. SSG is represented in Figure 9, which is a pilot living lab jointly created by ABB, Vaasan Sähköverkko (DSO), Elisa (communications) and University of Vaasa [39]. Real-time voltage and current measurements (IEC 61850 standard) recorded from the MV distribution network, from all four feeders at an HV/MV substation and three MV/LV substations comprising 20 measurement points in total. Measurements are sampled at 80 samples/cycle. In addition measurements of, active and reactive power, frequency, RMS voltages, currents etc. are received by GOOSE messages. Figure 10 represents SSG with Li-ion BESS integrated to the MV grid.

The base case scenario where SSG is simulated without BESS in the MV distribution system is shown in Figure 9. This approach enables us to record the active and reactive power flows at the HV/MV interface and active power flow of the WTG. The SSG WTG is of permanent magnet synchronous generator type, thereby allowing it to absorb or inject reactive power to 100% of its rated power. In this case, the reactive power control (QU-control) of the WTG is disabled, to record the original characteristics in the SSG without the operation of any flexible energy resources adhering to IEEE 1547–2018 [40] guidelines.

P_{WT} and Q_{WT} generation from the wind turbine is shown in Figure 11(a), where negative symbol denotes power generation. Figure 11(b) shows the active (P_{HV}) and reactive power (Q_{HV}) flow from the HV side of the HV/MV transformer. In the early part of the day, grid supplies power due to the reduced wind power generation and later it starts to consume power generated from SSG. The flexibilities provided by the reactive power control of the WTG is unused to record the system parameters in the base case scenario. V_{HV} and V_{MV}, the system voltages measured during the simulation, from the HV and MV side of the transformers respectively. The SSG as a grid-connected microgrid, proves to be a very stiff grid on the HV side with V_{HV} close to 1 pu. Whereas, the voltage in the MV side of the transformer is close to 0.94 pu (Figure 11(c)), which is well under the limitations commanded from the Fingrid's RPW. Hence, there exists a need from flexible energy sources to regulate system voltage at the MV grid, in the absence of OLTC. Hence, the following cases are defined to utilise the available flexibilities to stabilise voltage in the MV distribution system.

4.2 | Case 2: ANM flexibilities (WTG only)

In this case, the WTG's reactive power flexibility in the SSG is utilised to control voltage at the MV bus, adhering to the modified standards explained in Section 3. P_{WT} of the WTG is the recorded measurement data. However, Q_{WT} control of WTG system depends on the reactive power output capability based on QU-control calculations.

The flexibilities of QU-control from the WTG have been utilized to stabilise MV distribution system's voltages. The WTG absorbs reactive power in the system to its maximum possible value as defined by the ANM scheme determined in Section 3. Active and reactive power flows from the WTG is shown in Figure 12(a), where the instantaneous Q_{WT} is determined by Equation (5). The voltages at the HV and MV side of the HV/MV transformer in SSG is presented in Figure 12(b). Despite the maximum flexibility available from the QU-control of WTG, it is observed that the voltages in the MV side of the transformer, does not stay within limits defined by the ANM targets. Hence, further flexibilities are required in the network to regulate voltage at the MV distribution system.

4.3 | Case 3: ANM flexibilities (WTG and BESS)

Li-ion BESS and its integration in MV grid using power converters (bus J10*) are shown in Figure 10. BESS has been modelled based on the SOEC method as explained in Section 2. Li-ion BESS characteristics are presented in Table 1.

Due to its capability in both catering both active and reactive power requirements of the SSG, BESS controllers should include both P-control by regulating P_{BESS} and QU-control by regulating Q_{BESS}, there by satisfying the ANM requirements commanded by the MV distribution system in SSG. BESS internal control algorithms are described by Equations (7)–(9). Li-ion BESS active power control in the MV the distribution system is shown in Equation (7), which is primarily designed to P_{chg}, when the wind power generation exceeds load demand and P_{dis} during higher demand than its wind power production,

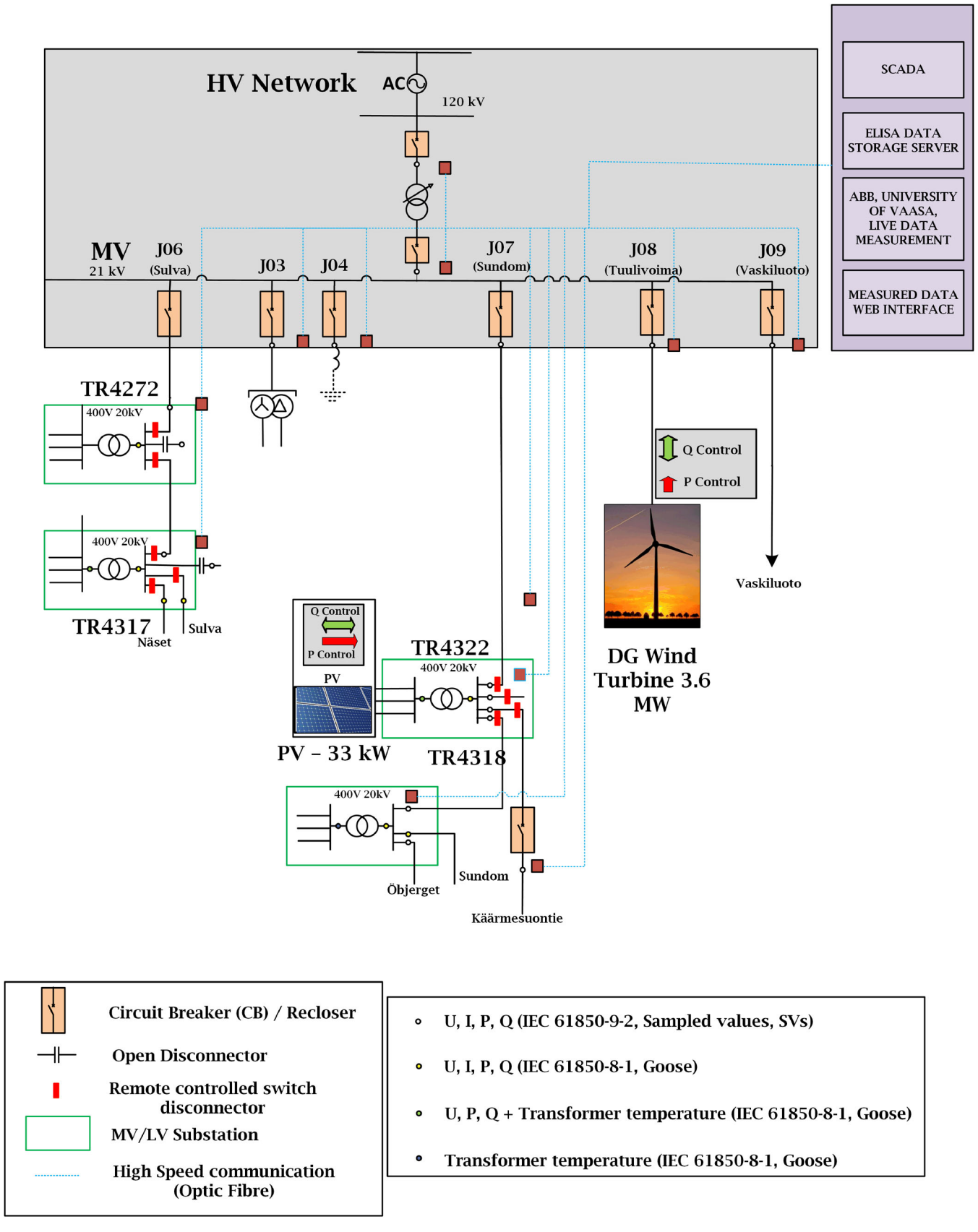

FIGURE 9 Existing SSG network

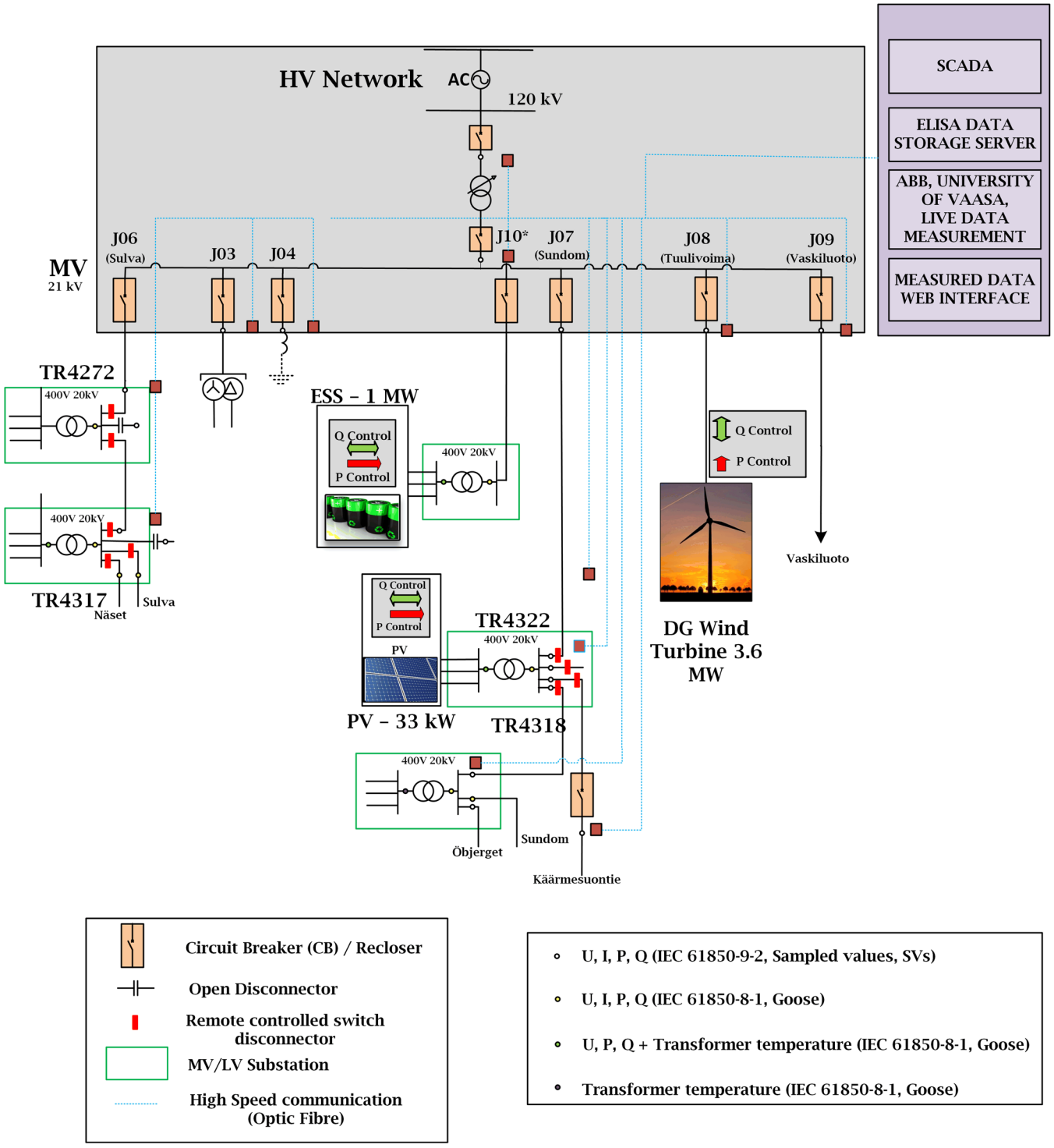

FIGURE 10 SSG with Li-ion BESS

which is controlled by the battery's *SoC* within their threshold SoC_{min} and SoC_{max}. Overall active power discharged by the BESS is defined by Equation (8) and the BESS is charged with a power of 500 kW as with a C-rate of 0.5 C as shown in Equation (9). Simulations are run by integrating Li-ion BESSs in the MV distribution system and their respective controllers are evaluated. Figure 13(a) presents active and reactive power of the BESS, following the commands set by Equations (7)–(9). During the beginning of the simulation P_{Load} is greater than P_{WT}. Hence, the BESS begins to discharge active power, with any reactive power flow due to the grid's reference set. However, during the course of the day, P_{WT} increases and is able to cater the load demand requirements and also capable of charging the BESS. Over this period, it is noted that the maximum reactive support from BESS is utilised due to its requirement to regulate MV bus voltage except the time during BESS charge. In that

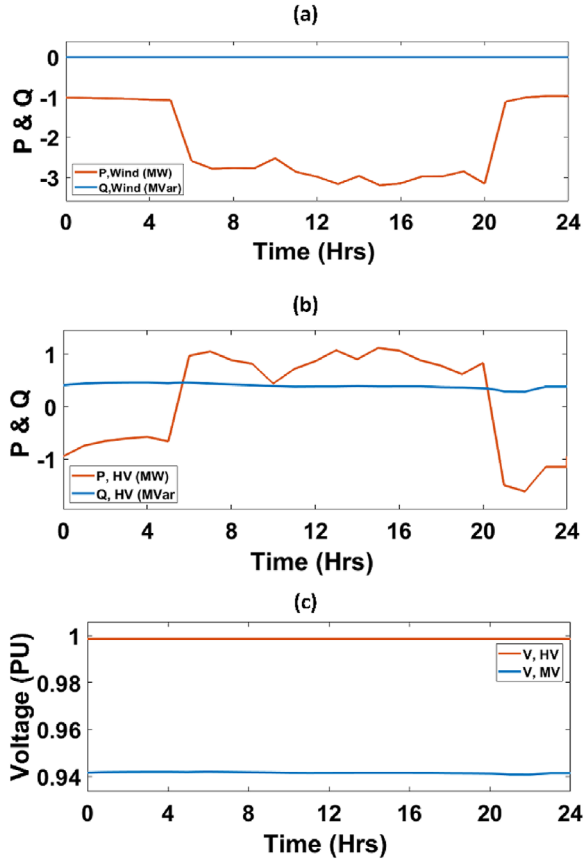

FIGURE 11 Case (1) results: (a) Active and reactive power flow at the HV side. (b) Active and reactive power of WTG. (c) Voltages in HV and MV grids

TABLE 1 Li-ion BESS characteristics

Lithium-ion battery characteristics	
Nominal DC voltage	525 V
Peak voltage	597 V
Cut-off voltage	397 V
Discharge energy(1C)	1 MWh
Nominal discharge current (1C)	2104 A

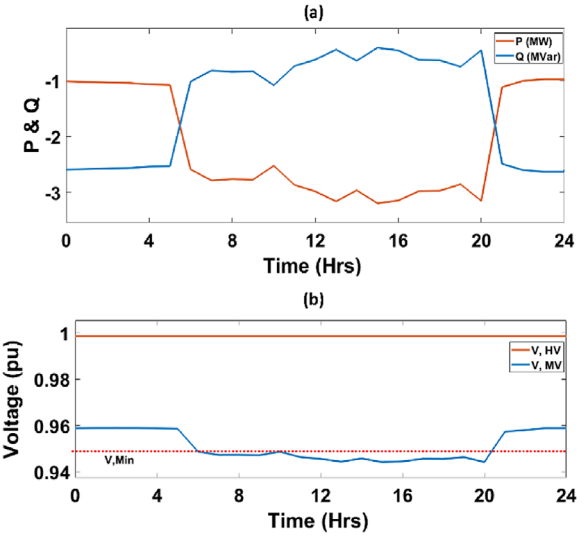

FIGURE 12 Case (2) results: (a) Active and reactive power of WTG. (b) Voltages in HV and MV grid

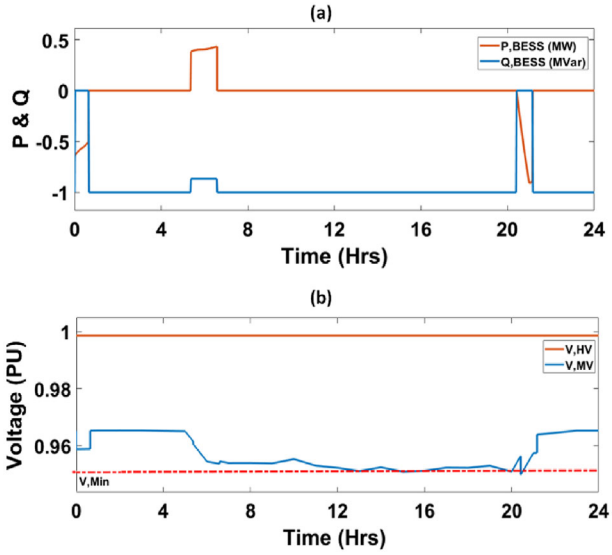

FIGURE 13 Case (3) results: (a) BESS active and reactive power (b) HV and MV voltages

instance, reactive power flow is controlled by Equation (6). MV and HV bus voltages are presented in Figure 13(b), where both the voltages are within the threshold values determined by the ANM control architecture. The primary advantage of adding the SOEC battery model to the SSG to design their controller principles is to understand the way battery as a component responds to the requirements presented by the grid. Figure 14 explains various battery characteristics on the DC side due to the demands exerted by the AC side of the power grid. BESS operates with a range of SoC_{min} and SoC_{max}, which is as shown in Figure 14(a), where it operates between 20% and 90% SoC accurately. Figure 14(b) shows the DC current characteristics on the battery, where P_{dis} operation does not exceed 1MW and P_{chg} happens at 500 kW. BESS voltage characteristics are shown in Figure 14(c), which provides an important set-point for control of power converters employed to integrate battery systems to the grid and Figure 14(d) presents the DC power characteristics. The PI-controllers representing control of the flexibilities from BESS and WTG are represented in Table 2.

When the BESS is subjected to the current profile in Figure 14(b), the temperature changes in the battery cell due to

TABLE 2 PI controller coeficients

Grid side controllers	*Kp*	*Ki*
P_{BESS}	0.005	1
Q_{BESS}	0.005	1
Q_{WT}	0.3974	0.9196

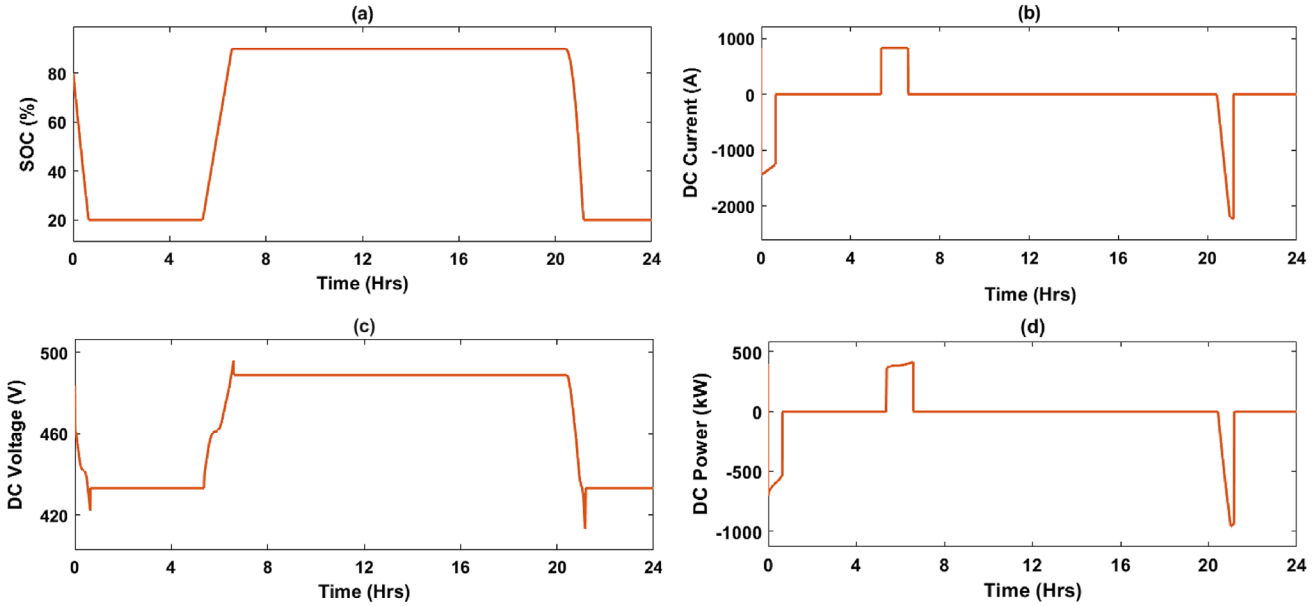

FIGURE 14 (a) Battery SoC; (b) Battery DC charge/discharge currents; (c) Battery SC voltage; (d) Battery DC power characteristics

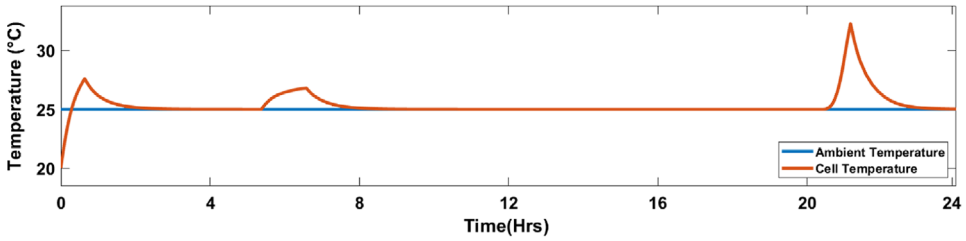

FIGURE 15 Battery cell operational temperature profile

the heat generated during its operation is represented in Figure 15. It is assumed that the ambient temperature is 25 °C. This result from the battery thermal model provides direct information on the effect of grid current requirements on the BESSs thermal characteristics. Hence, the SOEC battery model provides set points to design battery management systems, that is by considering both thermal and electrical characteristics of battery operation.

5 | CONCLUSION

Li-ion BESSs will play a dominant role as flexible energy sources for stationary grid applications because of their versatile nature, tending multi-objective applications in ANM schemes and their capability to participate in active and reactive power flexibility markets. However, the Li-ion BESSs are highly non-linear in performance with stringent safety requirements due to their characteristics. It is important to include the parameters affecting battery performance while designing grid-scale controllers for BESS to cater to the power system requirements. Hence, in this paper ANM control schemes were developed by utilising the second-order equivalent circuit battery model, an accurate representation of battery operations keeping the battery characteristics in safe operational areas. Li-ion BESS controls were designed to cater effective management of available flexibilities in the MV distribution system. Such studies allow validating the BESS-ANM control schemes and provide a detailed analysis on the impact of such load curves on the BESS performance attribute.

In future, more use cases will be added on to the existing multi-use scenarios of the BESS for managing flexibilities in a medium voltage distribution system, especially with respect to catering system frequency related challenges and the effects of Li-ion BESS aging will be included for smart grid applications.

ORCID

Chethan Parthasarathy https://orcid.org/0000-0002-2926-9367
Hossein Hafezi https://orcid.org/0000-0003-1859-6263

REFERENCES

1. Usman, M., Coppo, M., Bignucolo, F., Turr, R.: Losses management strategies in active distribution networks: A review. Electr. Power Syst. Res. 163(7), 116–132 (2018)

2. Christakou, K.: A unified control strategy for active distribution networks via demand response and distributed energy storage systems. Sustain. Energy, Grids Networks. 6, 1–6 (2016)
3. Palizban, O., Kauhaniemi, K., Guerrero, J.M.: Microgrids in active network management–Part II: System operation, power quality and protection. Renew. Sustain. Energy Rev. 36, 440–451 (2014)
4. Karagiannopoulos, S., et al.: Active distribution grids offering ancillary services in islanded and grid-connected mode. IEEE Trans. Smart Grid. 11(1), 623–633 (2020)
5. Christakou, K., Paolone, M., Abur, A.: Voltage control in active distribution networks under uncertainty in the system model: A robust optimization approach. IEEE Trans. Smart Grid. 9(6), 5631–5642 (2018)
6. Luo, E., et al.: Two-stage hierarchical congestion management method for active distribution networks with multi-type distributed energy resources. IEEE Access. 8, 120309–120320 (2020)
7. Calderaro, V., et al.: A smart strategy for voltage control ancillary service in distribution networks. IEEE Trans. Power Syst. 30(1), 494–502 (2015)
8. Mendonca, T.R.F., Green, T.C.: Distributed active network management based on locally estimated voltage sensitivity. IEEE Access. 7, 105173–105185 (2019)
9. Stecca, M., et al.: A comprehensive review of the integration of battery energy storage systems into distribution networks. IEEE Open J. Ind. Electron. Soc. 1(1), 1–1 (2020)
10. Li, C., et al.: Optimal OLTC voltage control scheme to enable high solar penetrations. Electr. Power Syst. Res. 160, 318–326 (2018)
11. Münderlein, J., et al.: Analysis and evaluation of operations strategies based on a large scale 5 MW and 5 MWh battery storage system. J. Energy Storage. 24(5), (2019)
12. Vazquez, S., et al.: Energy storage systems for transport and grid applications. IEEE Trans. Ind. Electron. 57(12), 3881–3895 (2010)
13. Hesse, H.C., et al.: Lithium-ion battery storage for the grid - A review of stationary battery storage system design tailored for applications in modern power grids. Energies. 2107, 10(12), (2017)
14. Müller, M.: Stationary Lithium-Ion Battery Energy Storage Systems A Multi-Purpose Technology. Ph.D. thesis, TUM (2018)
15. Lawder, M.T., et al.: Battery energy storage system (BESS) and battery management system (BMS) for grid-scale applications. Proc. IEEE. 102(6), 1014–1030 (2014)
16. Datta, U., Kalam, A., Shi, J.: Smart control of BESS in PV integrated EV charging station for reducing transformer overloading and providing battery-to-grid service. J. Energy Storage. 28, 101224, (2020)
17. Iurilli, P., Brivio, C., Merlo, M.: SoC management strategies in battery energy storage system providing primary control reserve. Sustain. Energy, Grids Networks. 19, 100230 (2019)
18. Datta, U., Kalam, A., Shi, J.: The relevance of large-scale battery energy storage (BES) application in providing primary frequency control with increased wind energy penetration. J. Energy Storage. 23(2), 9–18 (2019)
19. Wang, T., Cassandras, C.G.: Optimal control of multibattery energy-aware systems. IEEE Trans. Control Syst. Technol. 21(5), 1874–1888 (2013)
20. Bako, Z.N., et al.: Experiment-based methodology of kinetic battery modeling for energy storage. IEEE Trans. Ind. Appl. 55(1), 593–599 (2019)
21. Castaneda, M., et al.: A new methodology to model and simulate microgrids operating in low latitude countries. Energy Procedia. 157, 825–836 (2019)
22. Imran, R.M., Li, Q., Flaih, F.M.F.: An enhanced lithium-ion battery model for estimating the state of charge and degraded capacity using an optimized extended kalman filter. IEEE Access. 8, 208322–208336, (2020)
23. Kim, T., et al.: An on-board model-based condition monitoring for lithium-ion batteries. IEEE Trans. Ind. Appl. 55(2), 1835–1843 (2019)
24. Yang, J.: A closed-loop voltage prognosis for lithium-ion batteries under dynamic loads using an improved equivalent circuit model. Microelectron. Reliab. 100–101(7), 113459 (2019)
25. Nejad, S., Gladwin, D.T., Stone, D.A.: A systematic review of lumped-parameter equivalent circuit models for real-time estimation of lithium-ion battery states. J. Power Sources. 316, 183–196 (2016)
26. Meng, J., et al.: Overview of lithium-ion battery modeling methods for state-of-charge estimation in electrical vehicles. Appl. Sci. 8(5), 659 (2018)
27. El Sayed, M., et al.: Reduced-order electrochemical model parameters identification and soc estimation for healthy and aged li-ion batteries part i: parameterization model development for healthy batteries. IEEE J. Emerg. Sel. Top. Power Electron. 2(3), 659–677 (2014)
28. Parthasarathy, C., et al.: Modelling and simulation of hybrid pv & bes systems as flexible resources in smartgrids – sundom smart grid case. In: IEEE PES PowerTech Conference, Milan, Italy, pp. 1–6 (2019)
29. Parthasarathy, C., Hafezi, H., Laaksonen, H.: Lithium-ion bess integration for smart grid applications - ecm modelling approach. IEEE Power & Energy Society Innovative Smart Grid Technologies Conference (ISGT), Washington, DC, USA, (2020)
30. Arunachala, R., et al.: Inhomogeneities in large format lithium ion cells: A study by battery modelling approach. ECS Trans. 73(1), 201–212 (2016)
31. Nemounehkhah, B., et al.: Comparison and evaluation of state of charge estimation methods for a verified battery model. In: 2020 International Conference on Smart Energy Systems and Technologies (SEST), Istanbul, Turkey, pp. 1–6 (2020)
32. Kalogiannis, T., et al.: A comparison of internal and external preheat methods for NMC batteries. World Electr. Veh. J. 10(2), 1–16 (2019)
33. Laaksonen, H., et al.: Multi-objective active network management scheme studied in sundom smart grid with mv and lv connected der units. CIRED 2019, Madrid, Spain, (2019)
34. Sirviö, K., et al.: Controller development for reactive power flow management between dso and tso networks. IEEE PES Innovative Smart Grid Technologies Europe (ISGT-Europe), Bucharest, Romania, pp. 1–5 (2019)
35. Sirviö, K., Laaksonen, H., Kauhaniemi, K.: Active network management scheme for reactive power control. Cired Workshop 2018 on Microgrids and Local Energy Communities, Ljubljana, Slovenia, 7–8, (2020)
36. Sirvio, K., et al.: Prospects and costs for reactive power control in sundom smart grid. IEEE PES Innovative Smart Grid Technologies Conference Europe (ISGT-Europe), Sarajevo, Bosnia and Herzegovina, p. 1–6, (2018)
37. Laaksonen, H., Hovila, P., Kauhaniemi, K.: Combined islanding detection scheme utilising active network management for future resilient distribution networks. J. Eng. 2018(15), 1054–1060 (2018)
38. Panigrahy, N., et al.: Real-time phasor-emt hybrid simulation for modern power distribution grids. IEEE International Conference on Power Electronics, Drives and Energy Systems (PEDES), Trivandrum, India, p. 1–6 (2017)
39. Laaksonen, H.: Future-proof Islanding Detection Schemes in Sundom Smart Grid. 24th International Conference on Electricity Distribution (CIRED 2017) Glasgow, Scotland, pp. 12–15 (2017)
40. IEEE Standard Association, *IEEE Std. 1547–2018. Standard for Interconnection and Interoperability of Distributed Energy Resources with Associated Electric Power Systems Interfaces*. (2018)

How to cite this article: Parthasarathy, C., Sirviö, K., Hafezi, H., Laaksonen, H.: Modelling battery energy storage systems for active network management—coordinated control design and validation. *IET Renew. Power Gener.* 1–12 (2021).
https://doi.org/10.1049/rpg2.12174